

# UC San Diego

## UC San Diego Electronic Theses and Dissertations

### Title

A Microfluidic Device for the Study of Neutrophil Chemotaxis in 3D Environments

### Permalink

<https://escholarship.org/uc/item/9120t9xp>

### Author

Gorgen, Vivian Anne

### Publication Date

2016

Peer reviewed|Thesis/dissertation

UNIVERSITY OF CALIFORNIA, SAN DIEGO

A Microfluidic Device for the Study of Neutrophil Chemotaxis in 3D Environments

A Thesis submitted in partial satisfaction of the requirements for the degree  
Master of Science

in

Engineering Science (Mechanical Engineering)

by

Vivian Anne Gorgen

Committee in charge:

Professor Juan C. Lasheras, Chair  
Professor Juan Carlos Del Alamo  
Professor David Saintillan

2016

Copyright

Vivian Anne Gorgen, 2016

All rights reserved

The Thesis of Vivian Anne Gorgen is approved and it is acceptable in quality and form for publication on microfilm and electronically:

---

---

---

Chair

University of California, San Diego

2016

## TABLE OF CONTENTS

Signature Page.....	iii
Table of Contents.....	iv
List of Figures.....	vi
List of Tables.....	viii
Abstract of the Thesis.....	ix
1. Introduction.....	1
1.1. Cell Migration.....	3
1.2. Chemotaxis Index.....	3
1.3. HL-60 Cells.....	3
1.4. <i>In vitro</i> Methods for Studying Chemotaxis .....	4
1.5. Hydrogel.....	8
1.6. Standard Experimental Set Up.....	9
2. Methods.....	10
2.1. Design of the Device.....	10
2.1.1. Cover.....	10
2.1.2. Hydrogel.....	11
2.1.3. Spacer.....	11
2.1.4. Coverslip.....	11
2.1.5. PDMS Gasket.....	11
2.1.6. Viewing Window.....	11
2.2. Fabrication of the Device.....	12
2.2.1. Fabrication of Acrylic Parts.....	12
2.2.2. Fabrication of PDMS Gasket.....	12
2.2.3. Fabrication of Hydrogel Stamp.....	12

2.2.4. Fabrication of Hydrogel .....	13
2.3. HL-60 Cell Culture and Differentiation.....	14
2.4. Preparation of Collagen Gel.....	14
2.5. Operation and Experiment of the Device .....	15
2.6. Characterization of the Concentration Gradient .....	16
2.7. Chemotaxis Studies.....	16
2.8. Data Analysis.....	17
3. Results.....	18
3.1. Characterization of the Concentration Gradient.....	18
3.2. Chemotaxis Studies.....	23
4. Discussion.....	33
4.1. Characterization of the Concentration Gradient.....	33
4.2. Chemotaxis Studies.....	33
5. Conclusion.....	35
6. References.....	36

## LIST OF FIGURES

Figure 1.1. Advantages and limitations of common chemotaxis assays.....	5
Figure 1.2. Example of convective flow based gradient generator.....	6
Figure 1.3. Side and top view of diffusion based gradient generator.....	7
Figure 2.1. Exploded view of chemotaxis device.....	10
Figure 2.2. Exploded view of hydrogel fabrication components.....	13
Figure 2.3. Set up for hydrogel fabrication.....	14
Figure 3.1. Fluorescent images of 50 nM rhodamine diffusion in device over time (magenta = source, green = center, and red = sink).....	18
Figure 3.2. Average intensity in device over time with 50 nM rhodamine in source channel (dark blue lines indicate earlier time points and light blue lines indicate later time points).....	18
Figure 3.3. Slope of gradient in center channel over time with 50 nM rhodamine in source channel.....	19
Figure 3.4. Fluorescent images of 50 and 25 nM rhodamine (in media) diffusion in device over time (magenta = sink, green = center, and red = source).....	20
Figure 3.5. Average intensity in device over time with 50 nM rhodamine in source channel and 25 nM rhodamine (in media) in center channel (dark blue lines indicate earlier time points and light blue lines indicate later time points).....	20
Figure 3.6. Slope of gradient in center channel over time with 50 nM rhodamine in source channel and 25 nM rhodamine (in media) in center channel.....	21
Figure 3.7. Fluorescent images of 50 nM rhodamine and 25 nM rhodamine (in a collagen gel) diffusion in device over time (magenta = sink, green = center, and red = source).....	22
Figure 3.8. Average intensity in device over time with 50 nM rhodamine in source channel and 25 nM rhodamine (in a collagen gel) in center channel (dark blue lines indicate earlier time points and light blue lines indicate later time points).....	22
Figure 3.9. Slope of gradient in center channel over time with 50 nM rhodamine in source channel and 25 nM rhodamine (in a collagen gel) in center channel.....	23
Figure 3.10. Example brightfield image of dHL-60 cell trajectories following 60 minute exposure to 25 nM fMLP (condition #2).....	24
Figure 3.11. Example plots of dHL-60 cell trajectories over 60 minute time period: condition #1 (A), condition #2 (B), and condition #3 (C).....	26

Figure 3.12. dHL-60 cells migrated in a significantly higher velocity (in the direction of the gradient) when exposed to a stable, linear fMLP gradient generated by the device ( $p < 0.001$ ).....28

Figure 3.13. dHL-60 cells migrated in a significantly lower velocity (perpendicular to the direction of the gradient) when exposed to a stable, linear fMLP gradient generated by the device ( $p < 0.001$ ).....29

Figure 3.14. Condition #1 angle histogram shows dHL-60 cells migrated randomly when there is no fMLP present in the chemotaxis device.....30

Figure 3.15. Condition #2 angle histogram shows dHL-60 cells migrated with a median angle of  $42^\circ$  in the direction of the gradient when fMLP is incorporated into the collagen gel.....30

Figure 3.16. Condition #3 angle histogram shows dHL-60 cells migrated with a median angle of  $7.8^\circ$  degrees in the direction of the chemoattractant gradient when exposed to a stable, linear gradient in the device.....31

Figure 3.17. dHL-60 cells migrated in a significantly more directed manner when exposed to a stable, linear fMLP gradient generated by the device ( $p < 0.001$ ).....32



## LIST OF TABLES

Table 3.1. Chemotaxis device experimental test conditions.....	24
Table 3.2. Percentage of Motile Cells.....	27

## ABSTRACT OF THE THESIS

A Microfluidic Device for the Study of Neutrophil Migration in 3D Environments

by

Vivian Anne Gorgen

Master of Science in Engineering Sciences (Mechanical Engineering)

University of California, San Diego, 2016

Professor Juan C. Lasheras, Chair

Cell migration is an important cellular process in many physiological events such as embryogenesis, wound healing, cancer metastasis, and inflammation. Chemotaxis is a process in which cells migrate in the direction of a chemical gradient. This process can be observed in the immune response, in which leukocytes will migrate from the vasculature into inflamed tissue. Advancements in fabrication technologies have led to the development of many devices for studying *in vitro* chemotaxis. This thesis presents a

hydrogel device that establishes a chemical gradient to study chemotaxis. The device creates the gradient using diffusion and maintains the stable, linear gradient using flow. The gradient profile was characterized by monitoring the diffusion of rhodamine to determine that a stable gradient can be established in 40 minutes. Differentiated HL-60 (dHL-60) cells were used as a model cell type to interrogate the capabilities of the device. These cells migrated in a directed manner when exposed to an fMLP gradient for 60 minutes with a mean CI of 0.6479. Several biochemical and mechanical experimental parameters, such as pre-activation of the dHL-60 cells and collagen gel concentration, can be further optimized to increase the chemotaxis response of the cells. This device enables the study of cells in 2D and 3D environments and was fabricated with readily available manufacturing tools – allowing for prototyping for new applications.

## 1. INTRODUCTION

Cell migration plays a central role in many biological processes in human development from the beginning in embryogenesis, throughout life in the immune response, and in the end by controlled cell death. Misregulation of cell migration can lead to many chronic pathological conditions including cancer, atherosclerosis, and arthritis<sup>1</sup>. The immune system has an important regulatory role in the development of many chronic pathological conditions<sup>2</sup>. Leukocytes are one of the key players in the immune response.

Leukocytes, often referred to as white blood cells, are a broad family of immune cells consisting of eosinophils, neutrophils, basophils, monocytes, and lymphocytes<sup>2</sup>. These cells utilize migration for the process of immune surveillance, which allows the host to distinguish between materials that are supposed to be there (“self”) and those that are not (“non-self”). Leukocytes mainly circulate in the blood stream and monitor the human body for invading pathogens, which often initiates a process known as inflammation<sup>3</sup>.

Inflammation will cause leukocytes to migrate from the vasculature to the site of injury in a tissue. Endothelial cells, cells that line the inside of blood vessels, will become more adhesive to neutrophils circulating in the blood. The neutrophils will become transiently attached to the endothelial cell and will “roll” along the endothelium. Eventually, the neutrophil will adhere firmly to the endothelium and migrate through the blood vessel wall into the damaged tissue<sup>3</sup>.

This migration process is known as diapedesis and has two modes. Transcellular diapedesis occurs when neutrophils migrate directly through endothelial cells to reach inflamed tissue. Conversely, paracellular diapedesis occurs when neutrophils migrate in between endothelial cells to reach inflamed tissue<sup>4</sup>. In the inflamed tissue, neutrophils

can direct their migration towards the site of infection through a migration process known as chemotaxis<sup>5</sup>.

In the inflamed tissue (i.e. three dimensional (3D) environment), leukocyte migration is considered to be a low adhesive process that is mostly dependent on cytoskeleton flexibility. Conversely, in two dimensional (2D) environments, leukocyte migration is often described as adhesive – requiring leukocytes to activate integrin receptors. Since leukocytes adopt distinct migration modes depending on the external environment, understanding leukocyte migration has garnered much interest in the scientific community<sup>6</sup>.

One of the areas of interest is how mechanical forces, such as traction forces exerted by migrating cells, direct cellular function (since it is now believed that both mechanical forces and biochemical cues equally impact cellular function)<sup>7</sup>. Characterizing the mechanisms by which cells migrate and quantifying the forces exerted during migration can lead to a better understanding of how mechanical forces play a role in cell biology. This knowledge may enable the development of new implantable materials, drug treatments, or novel therapies<sup>8</sup>.

With the advancement of microscopy and fabrication technologies, the methods for studying directed cell migration, chemotaxis, has evolved from simple chambers separated by porous membranes to complex microfluidic devices. This thesis focuses on the development and characterization of a device for the study of neutrophil migration in response to a chemical gradient.

### 1.1. Cell Migration

Cell migration is an important cellular process for many physiological events. During embryogenesis, cells migrate to the appropriate location to form functional tissues and organs. In cancer metastasis, cancer cells migrate from the primary tumor to invade surrounding tissue. Leukocytes, also known as white blood cells, can migrate through the blood vessel to the site of inflammation to kill bacteria.

Cell migration is mediated by physical and chemical factors<sup>9</sup>. Some cells can sense extracellular chemical signals and direct their migration along the concentration gradient of the signal in a process known as chemotaxis<sup>10</sup>. On the other hand, cells can also migrate randomly in response to a chemical factor in a process known as chemokinesis<sup>11</sup>.

### 1.2. Chemotaxis Index

The chemotaxis index (CI) of a cell is an indicator of how well cells migrate towards a chemoattractant<sup>12</sup>. The CI of a cell can be calculated by taking the cosine of the angle between a line in the direction of the gradient and a line connecting the start and end point of the cell<sup>12</sup>. A CI of 1 indicates that the cell is migrating in the direction of the gradient while a CI of 0 suggests that a cell is migrating perpendicular to a chemical gradient<sup>12, 13</sup>. In other words, a CI of 0 suggests that the cell does not sense the chemoattractant.

### 1.3. HL-60 Cells

Leukocytes circulate in the blood and migrate through blood vessel walls to sites of inflammation in response to material released by bacteria<sup>14</sup>. Neutrophils, a type of leukocyte, follow gradients of formylated peptides released by bacteria to perform

phagocytosis as part of the immune response. Primary neutrophils can be harvested from blood or bone marrow, but cannot be sustained in culture or cyro-preservation for extended periods of time. As a result, the human promyelocytic leukemia (HL-60) cell line was developed as a model for studying neutrophil migration. HL-60 cells must be differentiated with dimethyl sulfoxide (DMSO) in order to express a neutrophil-like phenotype<sup>15</sup>.

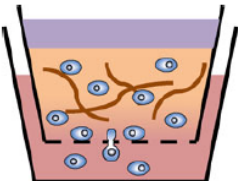
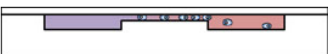
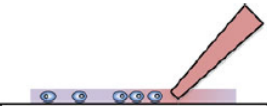
In response to a chemoattractant (migration-promoting agent), differentiated HL-60 cells (dHL-60) will adopt a polarized morphology (distinct front and back), which is essential for chemotaxis in mammalian cells<sup>16, 17</sup>. N-formyl-met-leu-phe (fMLP) is a chemoattractant known to induce superoxide production via NADPH oxidase, migration, and reorganization of actin in neutrophils<sup>18, 19</sup>. These responses are important in mounting an immune response<sup>18</sup>.

#### **1.4. *In vitro* Methods for Studying Chemotaxis**

There are several assays used to study mammalian cell chemotaxis such as the Boyden chamber, Zigmond chamber, and micropipette assay<sup>20</sup>. The Boyden chamber is used most commonly to study chemotaxis and consists of two compartments separated by a porous membrane. One compartment contains a cell suspension, which is placed in the second compartment containing a chemoattractant solution. Chemotactic activity is measured by quantifying the number of cells that migrate to the other side of the membrane or into the chemoattractant solution<sup>21</sup>. This assay has many advantages such as ease of use, scalability, and compatibility with cells in a 3D matrix. However, the Boyden chamber has limitations such as incompatibility with live imaging and inability to distinguish between chemotaxis (directed cell migration) and chemokinesis (random cell migration)<sup>20</sup>.

The Zigmond chamber addresses some of the limitations with the Boyden chamber. The Zigmond chamber consists of a Plexiglass slide with two fluid wells separated by a bridge. One well contains a chemotactic solution and the other well contains a buffer solution. A coverslip with cells is secured to the Plexiglass slide, which enables the formation of a linear concentration gradient and cell migration across the bridge<sup>22</sup>. Although the Zigmond chamber allows for live imaging, it is limited to 2D studies and hampered by low throughput<sup>20</sup>.

Similarly, the micropipette assay uses diffusion from a micropipette containing chemoattractant solution to create a concentration gradient allows for live imaging in 2D and 3D, but is low throughput and does not create a steady gradient<sup>20, 23</sup>.

	Advantages	Limitations
<p>Boyden chamber</p> 	<ul style="list-style-type: none"> <li>• Multiwell plate format that allows for a large number of screenings</li> <li>• Convenient and easy to use</li> <li>• System can be modified to introduce fluid flows</li> <li>• Cells can be embedded in a 3D matrix, which is a better mimic of <i>in vivo</i> microenvironments</li> </ul>	<ul style="list-style-type: none"> <li>• Population-based</li> <li>• Gradients are not well defined</li> <li>• Does not distinguish chemotaxis from chemokinesis</li> <li>• Not compatible with live cell imaging</li> <li>• Unknown membrane pore effect</li> </ul>
<p>Zigmond or Dunn chamber</p> 	<ul style="list-style-type: none"> <li>• Allows for video imaging</li> <li>• A nearly linear steady state gradient</li> </ul>	<ul style="list-style-type: none"> <li>• Poor reproducibility</li> <li>• 2D studies only</li> <li>• Short term experiments only</li> <li>• Low throughput</li> </ul>
<p>Micropipette assay</p> 	<ul style="list-style-type: none"> <li>• Compatible with optical microscope for the case of 2D studies</li> <li>• 3D studies possible</li> </ul>	<ul style="list-style-type: none"> <li>• Not a steady state gradient</li> <li>• Short-term experiments</li> </ul>

**Figure 1.1.** Advantages and limitations of common chemotaxis assays<sup>20</sup>

These chemotaxis assays generate chemical gradients by diffusion of attractant molecules through a medium and generally lack the ability to form a stable or adjustable gradient. The recent development of microfluidic technology offers many improvements over conventional chemotaxis assays including more physiologically relevant microenvironments, real time observation of cell movement, and decreased cellular



inputs. There are two types of microfluidic devices used for investigating chemotaxis: convective flow based microfluidic gradient generators and diffusion based microfluidic gradient generators<sup>24</sup>.

Convective flow based microfluidic devices generate concentration gradients by laminar flow of high and low concentration fluids through a series of serpentine channels that form a chemical gradient upon exit into a cell containing chamber<sup>20, 24</sup>. An important feature of these devices is that laminar flow on the micrometer scale allows for streams of miscible fluids to mix by diffusion without turbulent mixing – enabling the formation of repeatable concentration gradients<sup>25</sup>. This type of device has been used widely in the study of cell migration as it allows for rapid gradient formation (millisecond scale) and manipulation of gradient shape<sup>20, 24</sup>. However, flow based microfluidic gradient generators subject cells to fluid flow, which can cause three potential problems. First, shear stress has been shown to alter cell behavior. Secondly, the fluid flow will remove any autocrine or paracrine signals secreted by the cells. Lastly, in experiments with 3D matrices, the fluid flow may induce matrix remodeling<sup>20</sup>. Diffusion based microfluidic devices address some issues with flow based microfluidic devices.

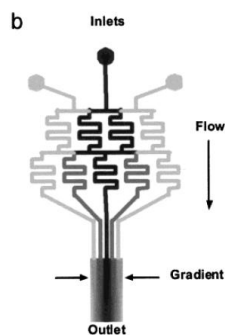


**Figure 1.2.** Example of convective flow based gradient generator<sup>26</sup>

Diffusion based microfluidic devices generate concentration gradients through molecular diffusion without exposing cells to fluid flow<sup>20</sup>. A gradient develops across a

region as molecules diffuse from “source” to “sink.” These devices are typically made with porous and permeable materials and consist of multiple channels, which physically isolate the cells from fluid flow – thus, addressing potential issues with flow based microfluidic devices. However, in devices where the source and sink have limited volume, the establishment of a stable concentration gradient can be slow and difficult to maintain over long periods of time<sup>20, 25</sup>. This is often mediated by manual pipeting or use of an external pump to maintain constant concentration in the source and sink.

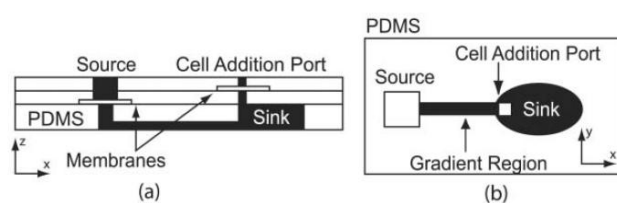


**Figure 1.3.** Side and top view of diffusion based gradient generator<sup>27</sup>

A hybrid microfluidic device has been developed that utilizes advantageous aspects of flow and diffusion based gradient generators. Similar to a diffusion based gradient generator, this device has a source and sink to enable the formation of a stable concentration gradient. However, unlike a diffusion based gradient generator, which relies on molecules to diffuse through a porous material to form a concentration gradient, this device uses flow to establish a gradient. Microcapillaries (20  $\mu\text{m}$  wide) connect the source, cell chamber, and sink, which will form a stable concentration gradient without exposing cells to unwanted flow<sup>28</sup>.

A hydrogel based microfluidic device developed by Shing-Yi Cheng et al<sup>29</sup> and Ulrike Haessler et al<sup>30</sup> utilizes the principles of diffusion based microfluidic gradient generators to study chemotaxis. The device consists of an agarose hydrogel with three channels: source, center, and sink. With the source and sink channels containing chemoattractant solution and blank buffer, respectively, molecules will diffuse across

the channels and establish a linear concentration gradient across the center channel. The center channel can have cells in 2D and 3D environments. This hydrogel based microfluidic device addresses many of the issues with commonly used methods for investigating chemotaxis including isolating cells from shear stress, compatibility with 2D and 3D microenvironments, and real time imaging. However, fabrication of the device requires soft lithography techniques, which are not easily accessible and can be costly. The microfluidic device described in this thesis uses readily available materials and equipment for fabrication – making this tool more adaptable for the research community.

### **1.5. Hydrogel**

As living cells are incorporated into microfluidic technology, conventional materials such as polydimethylsiloxane (PDMS) are being replaced with hydrogels that are more physiologically relevant and enable oxygen and nutrient exchange<sup>20</sup>. Hydrogels are naturally derived or synthetic polymeric networks swollen with large amounts of water<sup>31, 32</sup>. Agarose is a polysaccharide derived from seaweed. Agarose is soluble in boiling water and forms a gel when cooled to 31-36°C<sup>33</sup>. Agarose hydrogels have characteristics that are similar to living tissues such as rheological nature and water content, making it ideal for use in cell studies<sup>31</sup>.

There are several advantages to using agarose as a diffusion matrix in microfluidic devices. One of the most important features is that agarose is a biocompatible material that allows for the diffusion of incoming cell nutrients and growth factors and outgoing cellular waste. These conditions allow for high cell viability throughout the experimental testing. In addition, the diffusivity of most solutes in agarose gels is known to be similar to water, which suggests that the time needed to establish a gradient is short. Also, agarose is a thermally reversible hydrogel, allowing it to be easily

manipulated to create various features in the gel. Lastly, agarose is commercially available<sup>29, 33</sup>.

### **1.6. Standard Experimental Set Up**

A Leica DMI6000 B inverted microscope is used to characterize the device and conduct experiments. A camera is attached to the side port of the microscope to record images through Micro-Manager Open Source Microscopy Software. All experiments were conducted at 37°C.

All fluids were degassed prior to experiments and stored in plastic syringes during experiments. Fluids are pumped into the device using a NE-4000 Programmable 2 Channel Syringe Pump (New Era Pump Systems Inc.). Syringes are connected to the device with a female luer barb adapter, 1/16 inch inner diameter Tygon tubing, and shortened 20  $\mu$ L pipette tips wrapped with Teflon tape inserted into the device inlets. The device drains into a beaker through shortened 20  $\mu$ L pipette tips wrapped with Teflon tape and Tygon tubing inserted into the device outlets. The center channel (cell chamber) is plugged with shortened 20  $\mu$ L pipette tips wrapped with Teflon tape.

## 2. METHODS

### 2.1. Design of the Device

The device presented in this thesis was adapted from Shing-Yi Cheng et al<sup>29</sup> and Ulrike Haessler et al<sup>30</sup>. Briefly, the device consisted of an agarose hydrogel with three channels that is enclosed by a glass coverslip, clear acrylic, and PDMS gasket. Clear acrylic was selected so that any acquired images would not be occluded by the acrylic pieces. All acrylic pieces are 1.54 mm thick except the spacer, which is 6.35 mm thick. The device was secured with twelve 4-40 screws (1/2 inch length) and hex nuts. The overall dimensions of the device, 73 x 68 mm (L x W) were selected so the device could be secured to the microscope stage with existing stage platforms.

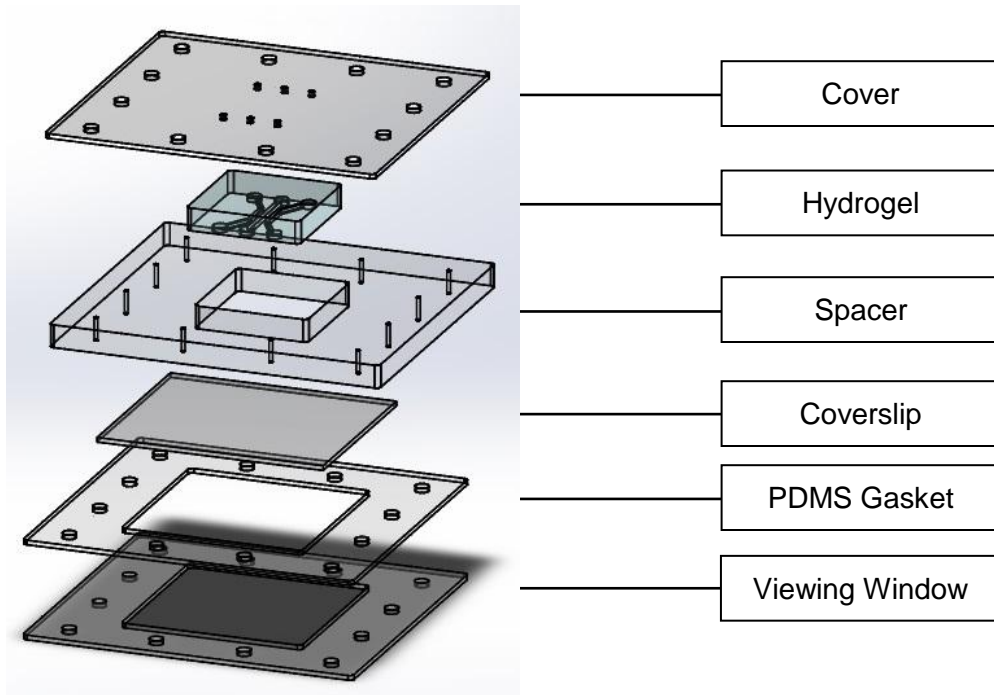


**Figure 2.1.** Exploded view of chemotaxis device

#### 2.1.1. Cover

The cover contains six holes that serve as inlet and outlet ports for the source, sink, and cell channels located in the hydrogel. The ports are 1.2 mm in diameter.

### 2.1.2. Hydrogel

The features in the agarose hydrogel were cast using a stamp. The hydrogel is approximately 25 x 25 x 6.35 mm (L x W x H). The source and sink channels are 18.92 x 0.8 x 1 mm (L (path length) x W x H). The cell chamber (center channel) is 17 x 1 x 1 mm (L x W x H). The spacing between all channels is 1 mm.

### 2.1.3. Spacer

The spacer has a 25 x 25 mm cut out which is used to fabricate the hydrogel channels and aids in aligning inlet/outlet ports.

### 2.1.4. Coverslip

The glass coverslip used was commercially available from Fisher Scientific (Catalog # 12-544F) with the following dimensions, 45 x 50 x 1.5 mm (L x W x H). The coverslip was is in direct contact with the channels in the hydrogel, which enables imaging of cells in the cell chamber (center channel).

### 2.1.5. PDMS Gasket

The PDMS gasket has similar dimensions to the viewing window (see below) and secures the glass coverslip to the hydrogel.

### 2.1.6. Viewing Window

The viewing window has a 40 x 40 mm (L x W) cut out which allows microscope objectives of varying sizes to view the cell chamber (center channel). The viewing window in this device is compatible with objectives that have magnifications ranging from 2.5x to 63x. The large viewing window enabled macroscopic studies with 30-50 cells in

view and microscopic studies with a single cell in view. The characterization studies outlined in this thesis used the 2.5x lens and the chemotaxis studies used a 5x lens.

## **2.2. Fabrication of the Device**

### **2.2.1. Fabrication of Acrylic Parts**

All acrylic parts were cut with a laser cutter (LaserCAMM) available at the MAE Design Studio at UCSD.

### **2.2.2. Fabrication of PDMS Gasket**

PDMS gaskets were made with Sylgard 184 Silicone Elastomer Kit (Dow Corning). The base and curing agent were combined 9:1 by weight to achieve an approximate total weight of 22.5 grams. The mixture was mixed at 2000 RPM for 3.5 minutes. The mixture was poured in a 100 mm Petri dish and placed in a vacuum chamber for 30 minutes. The Petri dish containing PDMS was incubated at 37°C overnight. The shape and features of the acrylic viewing window were traced onto the cured PDMS and cut to shape with a razor blade.

### **2.2.3. Fabrication of Hydrogel Stamp**

The hydrogel stamp was fabricated using a 3D printer and CNC machine. 3D printed parts were printed using a 3D Systems ProJet 3510 HD printer with VisiJet M3 Crystal made available by the MAE Design Studio at UCSD. Aluminum machined stamps were fabricated by the UCSD Machine Shop located at EBU 2 B-31 using a Hass VF-0 CNC machine.

#### 2.2.4. Fabrication of Hydrogel

The hydrogel was 3.5% (w/v) agarose (Lonza NuSieve GTG Agarose) in phosphate buffered saline (PBS). To prepare the agarose hydrogel, 0.7 grams of agarose was combined with 20 mL of PBS in a 100 mL glass beaker. The solution was microwaved for 25 seconds total – increments of 15, 5, and 5 seconds. The agarose solution was stored on a 105°C hot plate until use. The spacer was adhered to the stamp using vacuum grease. Approximately 3.5 mL of agarose was pipetted into the 25 x 25 mm cut out in the center of the stamp – all bubbles were removed from the solution using a pipette.

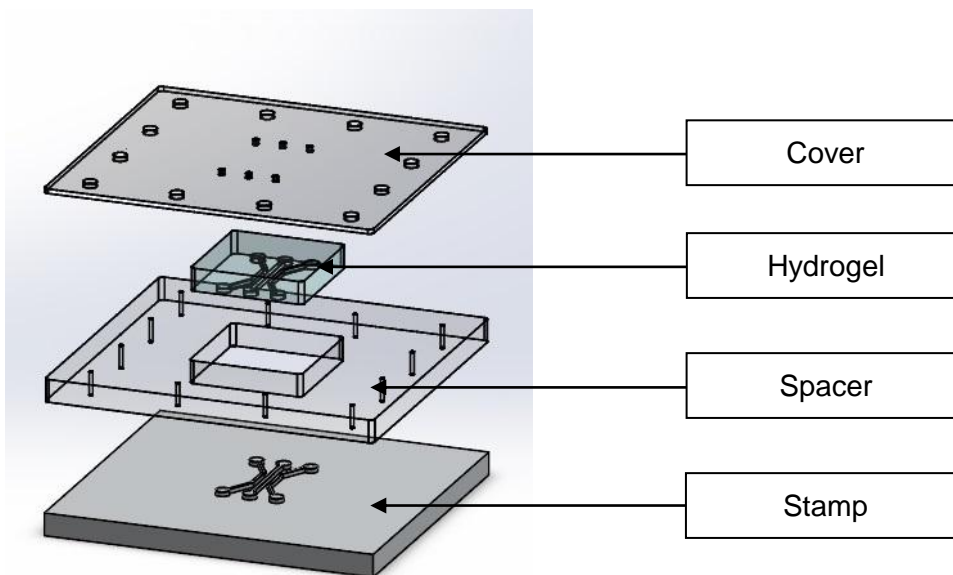


**Figure 2.2.** Exploded view of hydrogel fabrication components

The acrylic cover was placed on top of the agarose solution and four 4 x 40 screws were used to align the cover and spacer. Six 20  $\mu$ L pipette tips were inserted into the agarose through the ports in the cover. This allowed for the fluid inlet and outlet ports to be pre-formed in the hydrogel, which minimizes the amount of debris in the device



during use. Following a 15 minute incubation at room temperature, the hydrogel was removed from the stamp and stored in Roswell Park Memorial Institute (RPMI) 1650 plus L-glutamine media with 25 mM HEPES (ThermoFisher Scientific Catalog # 11875093) at 4°C until use.



**Figure 2.3.** Set up for hydrogel fabrication

### **2.3. HL-60 Cell Culture and Differentiation**

HL-60 cells were cultured by Joshua Francois (Lasheras group) according to protocols described by A. Millius and Orion D. Weiner [34]. Briefly, HL-60 cells were cultured in 100 mm cell culture treated Petri dishes with RPMI 1650 plus L-glutamine media with 25 mM HEPES, 15% fetal bovine serum (FBS), and 1% penicillin-streptomycin. Cells were maintained at 37°C and 5% CO<sub>2</sub> in a standard tissue culture incubator. HL-60 cells were differentiated into dHL-60 cells using dimethyl sulfoxide (DMSO). DMSO was added to the culture media in order to achieve a 1.3% DMSO concentration. Cells were differentiated for 4 days prior to experimentation.

### **2.4. Preparation of Collagen Gel**

dHL-60 cells were centrifuged at 3500 RPM for 10 minutes and resuspended in 62 nM fMLP (in RPMI) to achieve a 93,000 cells/mL suspension with a final fMLP concentration of 25 nM. 151  $\mu$ L of cell suspension and 5  $\mu$ L of 1 M NaOH were

combined in an Eppendorf tube. 219  $\mu\text{L}$  of 3.42 mg/mL type 1 rat tail collagen (Corning) was added to the Eppendorf tube and thoroughly mixed with a pipette. The collagen solution was added to the center channel of the device with a 20  $\mu\text{L}$  pipette. Collagen solution was added into the center channel until solution was observed exiting the outlet port and there are no bubbles present in the channel. All solutions were stored in ice until use. The collagen solution will form a gel in approximately 30 minutes at 37°C.

## **2.5. Operation and Experiment of the Device**

All liquids used in experiments were degassed in a vacuum chamber for at least 4 hours the day before an experiment and for at least 1 hour the day of an experiment.

The device was assembled by placing a coverslip onto the spacer, ensuring that the coverslip edges do not interfere with the screw threads. The PDMS gasket and viewing window were placed on top of the coverslip and secured to the spacer using twelve 4x40 screws.

The agarose hydrogel equilibrates to room temperature in RPMI media. Once the hydrogel has reached room temperature, it is dried with lint free tissue and placed into the cut out of the spacer, ensuring that the channels are in contact with the coverslip. The cover was placed onto the spacer and secured using hex nuts.

The source and sink channels (side channels) were checked for flow by pipetting degassed RPMI media into each channel using a 20  $\mu\text{L}$  pipette. Once flow was observed in the side channels and all bubbles were removed, the collagen gel was added to the center channel and plugged with 20  $\mu\text{L}$  pipette tips. The device was placed onto the microscope stage.

The flow rate on the syringe pump was initially set to 50  $\mu\text{L}/\text{min}$  to prime the tubing and device and later reduced to 20  $\mu\text{L}/\text{min}$ . The outlet tubing was initially

connected to a 10 mL syringe and filled with RPMI media. Once fluid flow was observed in the outlet ports, the outlet tubing was inserted into the outlet port and the syringe was disconnected from the outlet tubing. The outlets drained into a beaker.

## **2.6. Characterization of the Concentration Gradient**

The formation of the concentration gradient was characterized by monitoring the diffusion of a fluorescent dye in the device over time. Rhodamine is a fluorescent dye with a molecular weight of 566.99 g/mol (Fisher Scientific Catalog # AC446971000). Rhodamine was selected because it does not require conjugation to another species to emit fluorescence. Additionally, since the molecular weight of rhodamine is similar to the molecular weight of fMLP (437.55 g/mol), these experiments would not underestimate the amount of time needed to establish a linear concentration gradient in the device.

The source and sink channels were connected to syringes with 50 nM rhodamine and RPMI media, respectively. The center channel was filled with RPMI media +\ 25 nM rhodamine or collagen solution. Images were acquired using brightfield and fluorescent (TRITC) microscopy every 2 minutes with a 2.5x lens.

## **2.7. Chemotaxis Studies**

In order to examine how dHL-60 cells migrated in response to a chemoattractant gradient in the device, the source and sink channels were connected to syringes with 50 nM fMLP and RPMI media, respectively. The center channel contained a collagen solution with dHL-60 cells (as described previously). The device was placed on the microscope stage at 37°C to allow the collagen gel and chemoattractant gradient to form. Images were acquired using bright field microscopy every 2 minutes with a 5x lens.

## 2.8. Data Analysis

Custom MATLAB scripts (MathWorks) developed by Professor Lasheras's lab were used to analyze the acquired images. For characterization experiments, MATLAB was used to average the intensity of each image acquired to show the average intensity in the device over time. In addition, the slope of the intensity in the center channel was calculated to determine when the gradient in the center channel appeared to be linear.

For chemotaxis studies, MATLAB identified and tracked the centroid of the cells over time. Cells were considered motile if the magnitude of displacement at the end of the experiment was larger than 5  $\mu\text{m}$ . The percentage of motile cells is defined as:

$$\% \text{ motile cells} = \frac{\text{number of cells with displacement magnitude} > 5 \mu\text{m}}{\text{total number of cells}} \times 100$$

In addition, the velocity was calculated for all cells that were tracked by MATLAB. Similarly, unlike the percentage of motile cells analysis, the velocity analysis does not exclude cells with displacements less than 5  $\mu\text{m}$ . For this analysis, the X and Y-directions are parallel and perpendicular to the chemoattractant gradient, respectively. The velocity reported uses the cell's displacement over 60 minutes.

Lastly, the chemotaxis index (CI) was calculated for all cells that were tracked by MATLAB. Unlike the percentage of motile cells analysis, the CI analysis does not exclude cells with displacements less than 5  $\mu\text{m}$ . The CI values reported uses the cell's initial (t=0 min) and final position (t=60 min).

For each experiment, the first time point is defined as the time at which the gradient began to stabilize i.e. appear linear.

### 3. RESULTS

#### 3.1. Characterization of the Concentration Gradient

The concentration gradient was first characterized with 50 nM rhoadamine in the source channel and RPMI media in the center and sink channel.

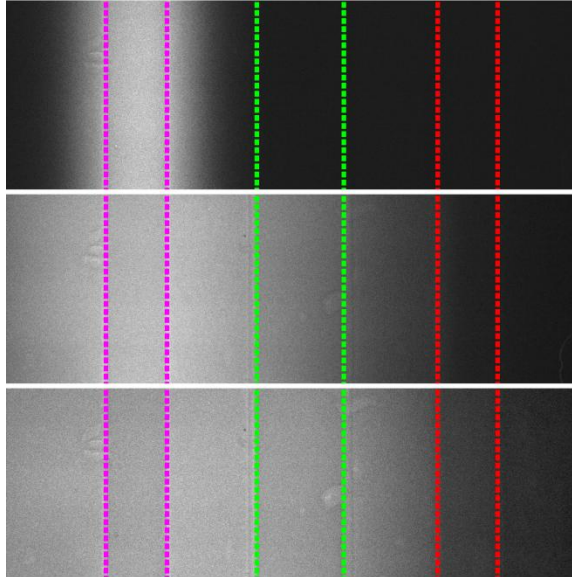


**Figure 3.1.** Fluorescent images of 50 nM rhodamine diffusion in device over time (magenta = source, green = center, and red = sink)

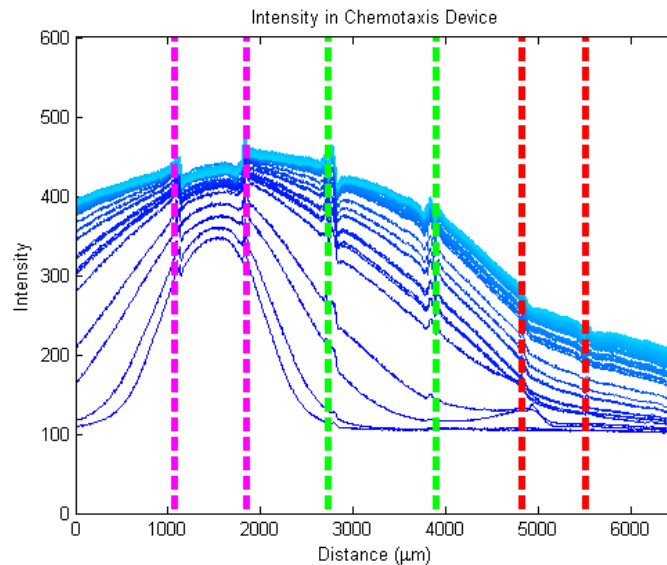


**Figure 3.2.** Average intensity in device over time with 50 nM rhodamine in source channel (dark blue lines indicate earlier time points and light blue lines indicate later time points)

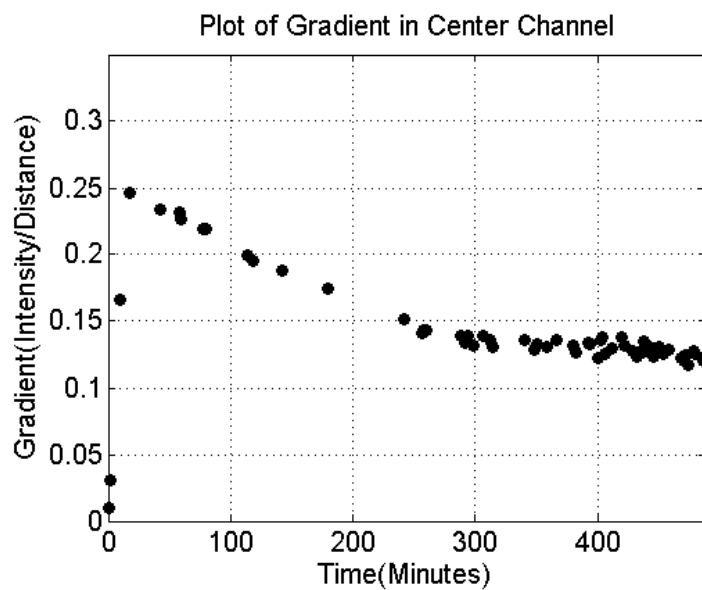


**Figure 3.3.** Slope of gradient in center channel over time with 50 nM rhodamine in source channel

When the source channel was filled with 50 nM rhodamine and the center and sink channels were filled with RPMI media, the gradient in the center channel appeared to stabilize in approximately 300 minutes and remained stable for at least 200 minutes.

In order to reduce the time needed for a stable gradient to form, the device was characterized with 50 nM rhodamine in the source channel, 25 nM rhodamine (in RPMI) in the center channel, and RPMI media in the sink channel.

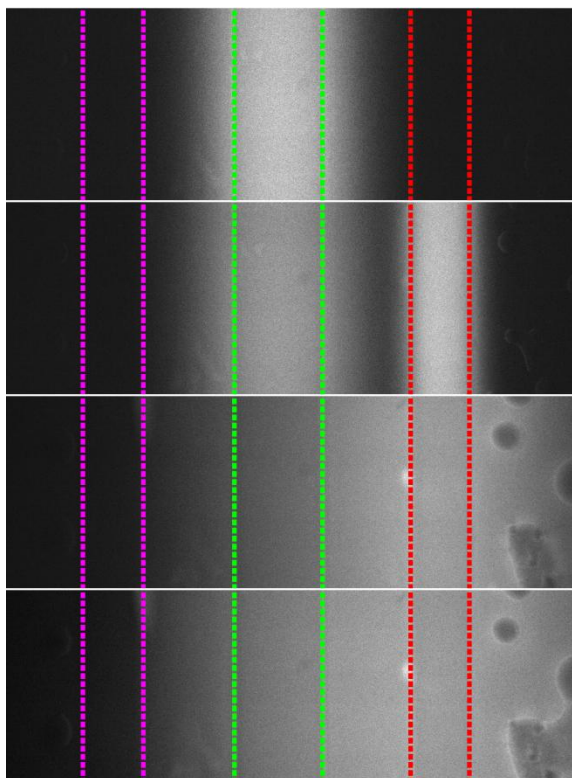


**Figure 3.4.** Fluorescent images of 50 and 25 nM rhodamine (in media) diffusion in device over time (magenta = sink, green = center, and red = source)

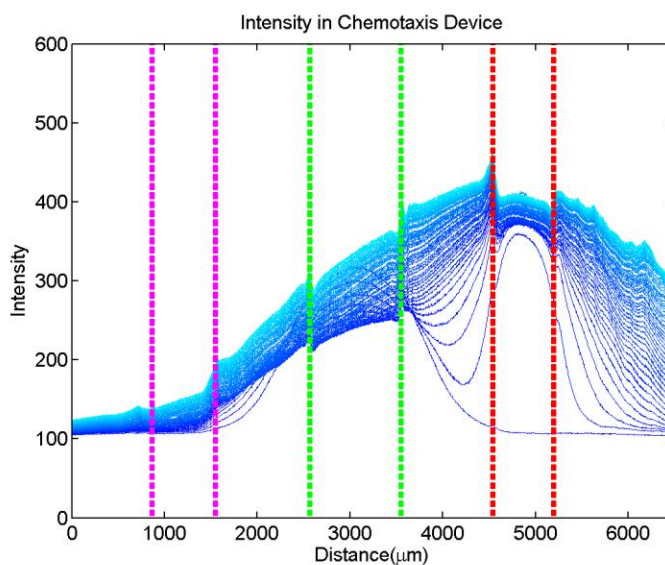


**Figure 3.5.** Average intensity in device over time with 50 nM rhodamine in source channel and 25 nM rhodamine (in media) in center channel (dark blue lines indicate earlier time points and light blue lines indicate later time points)

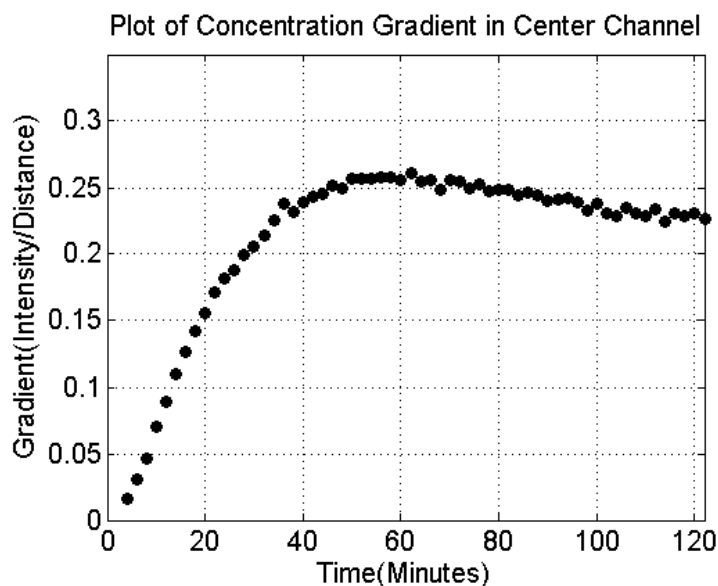


**Figure 3.6.** Slope of gradient in center channel over time with 50 nM rhodamine in source channel and 25 nM rhodamine (in media) in center channel

When the source channel was filled with 50 nM rhodamine and the center was filled with 25 nM rhodamine (in media), the gradient in the center channel appeared to stabilize at approximately 40 minutes and remained stable for at least 80 minutes.

Since chemotaxis experiments use a collagen gel in the center channel, the device was also characterized with 50 nM rhodamine in the source channel, a collagen gel with 25 nM rhodamine in the center channel, and RPMI media in the sink channel.



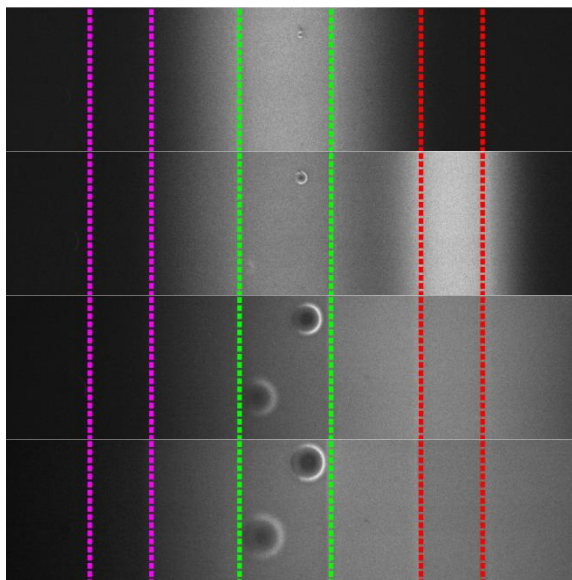


**Figure 3.7.** Fluorescent images of 50 nM rhodamine and 25 nM rhodamine (in a collagen gel) diffusion in device over time (magenta = sink, green = center, and red = source)

Note: Bubbles formed in the collagen gel (center channel) over time. As a result, the intensity was averaged in the region between the bubbles.

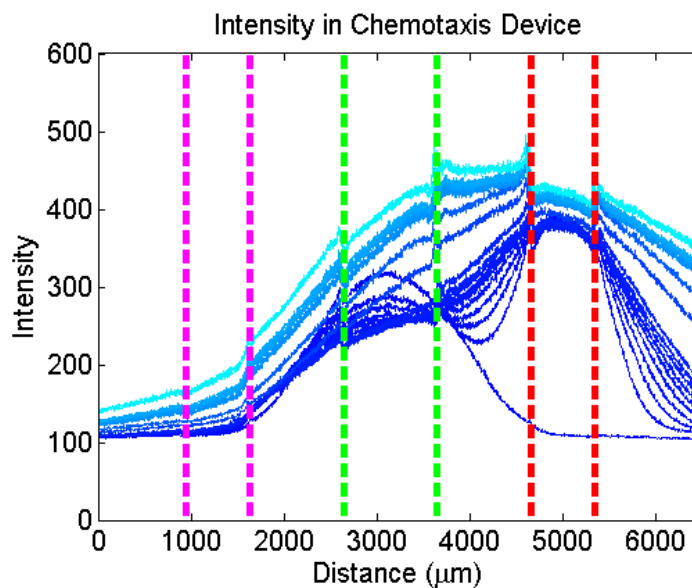


**Figure 3.8.** Average intensity in device over time with 50 nM rhodamine in source channel and 25 nM rhodamine (in a collagen gel) in center channel (dark blue lines indicate earlier time points and light blue lines indicate later time points)

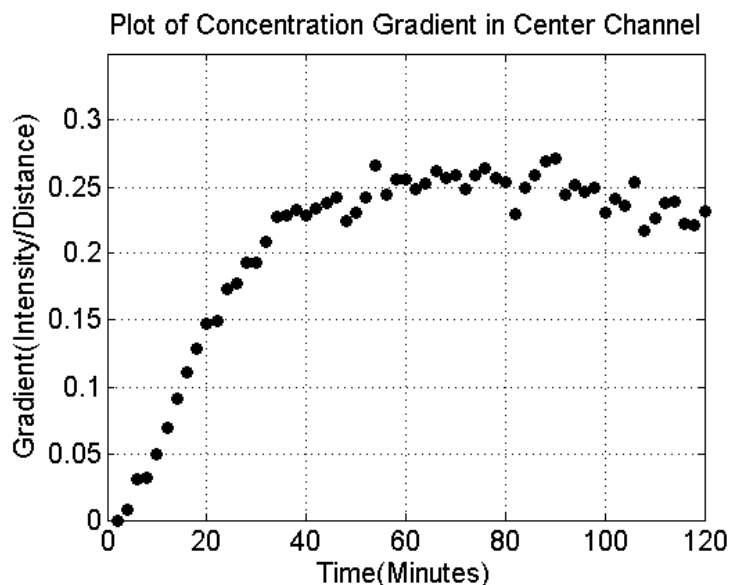


**Figure 3.9.** Slope of gradient in center channel over time with 50 nM rhodamine in source channel and 25 nM rhodamine (in a collagen gel) in center channel

When the source was filled with 50 nM rhodamine and the center channel was filled with a 25 nM rhodamine in a collagen gel, the gradient in the center channel appeared to stabilize at 40 minutes and remained stable for at least 80 minutes. Based on these results, chemotaxis experiments used collagen gels with a final fMLP concentration of 25 nM. Since the collagen solution takes approximately 30 minutes to form a gel and the gradient takes approximately 40 minutes to stabilize, the collagen solution formed a gel in the device while the gradient stabilized. For all chemotaxis experiments, the first time point was defined at 40 minutes.

### 3.2. Chemotaxis Studies

The migration of dHL-60 cells in the chemotaxis device was examined under various conditions. As a control condition (condition #1), dHL-60 cells were placed in the device with no fMLP present. In addition, since fMLP was introduced into the collagen

gel to decrease the gradient stabilization time from 300 minutes to 40 minutes, dHL-60 cells were placed in the device with fMLP in the collagen gel to evaluate whether or not this impacted cell migration (condition #2). The final test condition (condition #3) exposed the cells to a gradient of fMLP.

**Table 3.1.** Chemotaxis device experimental test conditions.

Condition	Name	Source Channel	Center Channel	Sink Channel
1	no fMLP	RPMI	Collagen gel (no fMLP)	RPMI
2	25 nM fMLP	RPMI	Collagen gel (25 nM fMLP)	RPMI
3	25 nM fMLP + gradient	50 nM fMLP	Collagen gel (25 nM fMLP)	RPMI

Brightfield imaging was optimized to focus on cells with a bright center to facilitate trajectory analysis. MATLAB code was used to number and track identified cells.

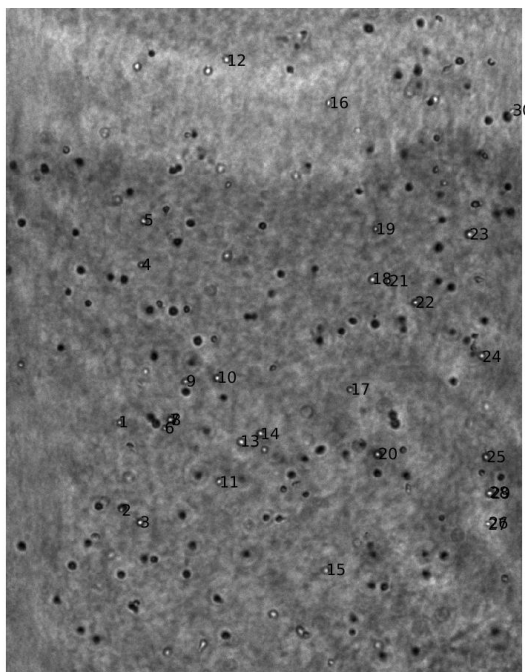


**Figure 3.10.** Example brightfield image of dHL-60 cell trajectories following 60 minute exposure to 25 nM fMLP (condition #2)

Additional analysis was performed on the sub population of cells whose trajectories were greater than 5  $\mu\text{m}$  at the end of the experiment. These cell paths were plotted on a Cartesian coordinate system to examine each cell's trajectory over a 60 minute time period with the origin representing the cell's initial position. For experiments with an fMLP gradient, RPMI and 50 nM fMLP are on the left and right of the plot, respectively.

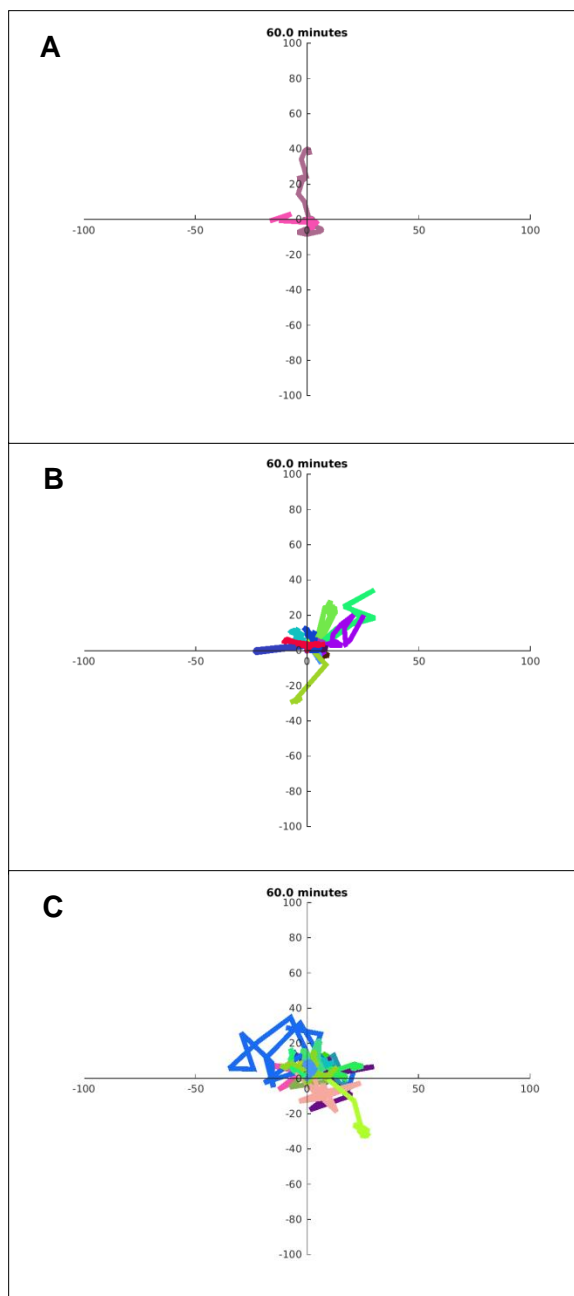


**Figure 3.11.** Example plots of dHL-60 cell trajectories over 60 minute time period: condition #1 (A), condition #2 (B), and condition #3 (C)

For condition #1, the average percentage of motile cells was 47.04%. The standard deviation and relative standard deviation (RSD) was not calculated for this condition because there were only two experimental replicates. For condition #2 (3

experiments), the average percentage of motile cells was  $52.90 \pm 21.34\%$ . For condition #3 (3 experiments), the average percentage of motile cells was  $62.23 \pm 22.62\%$ . An unpaired t-test indicates that the difference between the percentage of motile cells in condition #2 and #3 is not statistically significant ( $p$ -value = 0.63). This result was not unexpected since the cells are exposed to fMLP in both conditions, which would activate the cells to move.

**Table 3.2.** Percentage of Motile Cells

Condition	Average (%)	Standard Deviation (%)	RSD (%)
1	47.04	NA <sup>A</sup>	NA <sup>A</sup>
2	52.90	21.34	40.35
3	62.23	22.62	36.35

<sup>A</sup>The standard deviation and %RSD was not calculated for condition #1 because there were only two experimental replicates.

For all three test conditions, the total displacement for 60 minutes was used to determine the velocity for each cell. In the X-direction (parallel to the direction of the gradient), the mean velocity for condition #1 (64 cells), #2 (114 cells), and #3 (109 cells) was calculated to be -0.013, 0.039, and 0.064  $\mu\text{m}/\text{min}$  (outliers identified in MATLAB (see **Figure 3.12**) were not excluded in the mean velocity calculation. A Wilcoxon rank sum test was used to determine if the difference between the three test conditions were statistically significant ( $\alpha = 0.05$ ). When condition #2 and #3 were compared to condition #1, the  $p$ -values were much less than 0.001. This demonstrated that in the presence of fMLP, the dHL-60 cells moved at a higher velocity. This is an expected result since dHL-60 cells will move in response to a chemoattractant. However, when condition #2 and #3 were compared, the  $p$ -value was much less than 0.001. This showed that although the dHL-60 cells migrated when fMLP was incorporated into the collagen gel (condition #2), the cells migrated, in a direction parallel to the gradient, at a significantly higher velocity

when exposed to a stable, linear chemoattractant gradient generated by the device (condition #3).

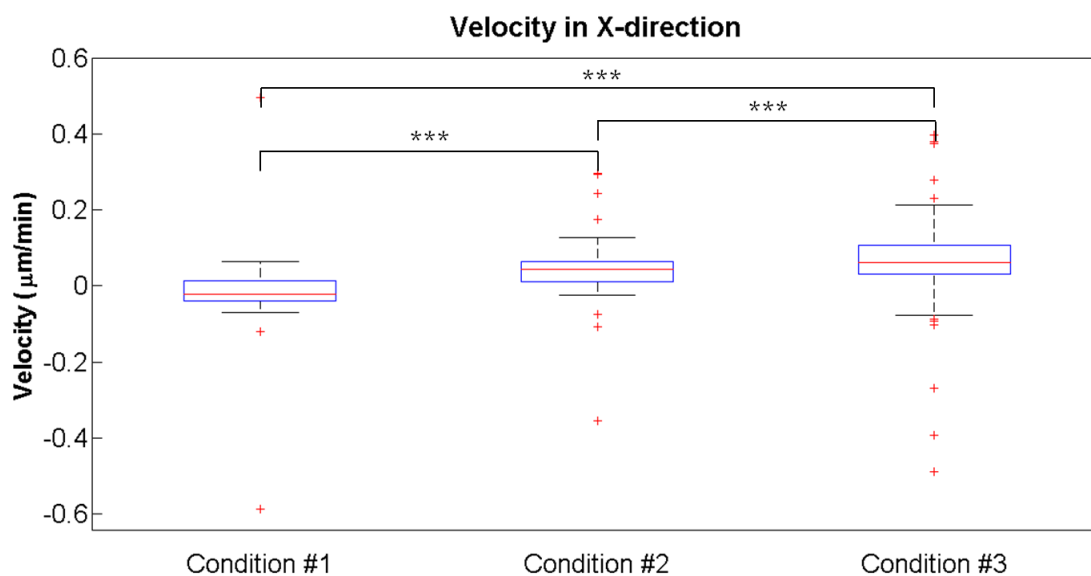


**Figure 3.12.** dHL-60 cells migrated in a significantly higher velocity (in the direction of the gradient) when exposed to a stable, linear fMLP gradient generated by the device ( $p < 0.001$ )

For all three test conditions, the total displacement at 60 minutes was used to determine the velocity for each cell. In the Y-direction (perpendicular to the direction of the gradient), the mean velocity for condition #1 (64 cells), #2 (114 cells), and #3 (109 cells) was calculated to be 0.012, 0.047, and 0.003  $\mu\text{m}/\text{min}$  (outliers identified in MATLAB (see **Figure 3.13**) were not excluded in the mean velocity calculation). A Wilcoxon rank sum test was used to determine if the difference between the three test conditions were statistically significant ( $\alpha = 0.05$ ). When condition #2 and #3 were compared, the p-value was much less than 0.001. This demonstrated that the cells in Condition #3, which were exposed to a stable, linear gradient, had a significantly lower velocity in the direction perpendicular to the chemoattractant gradient.

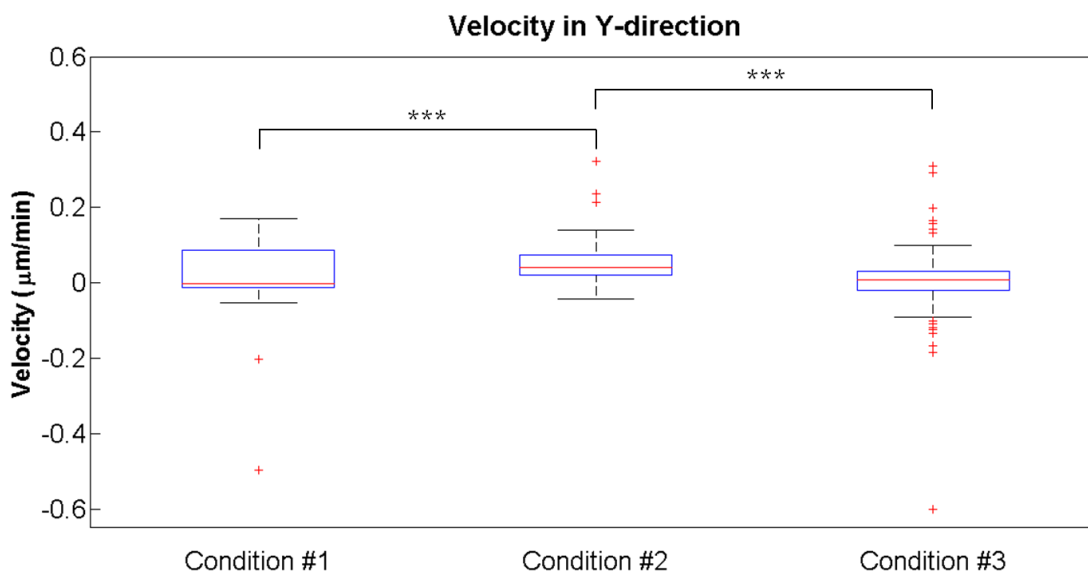


**Figure 3.13.** dHL-60 cells migrated in a significantly lower velocity (perpendicular to the direction of the gradient) when exposed to a stable, linear fMLP gradient generated by the device ( $p < 0.001$ )

Angle histograms were generated to show the angle of each cell's trajectory at the final time point ( $t = 60$  minutes). An Omnibus test showed that condition #1 had a uniform distribution ( $p$ -value = 0.9) while condition #2 and #3 did not have a uniform distribution ( $p$ -value  $< 0.001$ ). The weighted median angle (weights displacement of each cell) for condition #2 and #3 were  $42^\circ$  and  $7.8^\circ$ , respectively. As shown in **Figure 3.14**, condition #1 showed a uniform distribution of angles indicating that the cells are randomly moving. However, condition #2 showed that with fMLP incorporated into the collagen gels, the cells traveled with a median angle of  $42^\circ$  from the direction of the chemoattractant gradient (**Figure 3.15**). More importantly, condition #3 demonstrated that with a stable, linear fMLP gradient, the cells migrated with a median angle of  $7.8^\circ$  from the direction of the chemoattractant gradient (**Figure 3.16**). This demonstrates that the dHL-60 cells are migrating in a more directed manner in condition #3. For



experiments with an fMLP gradient, RPMI and 50 nM fMLP are on the left and right of the plot, respectively.

Instantaneous Angle Histogram at t = 60 minutes (Condition #1)

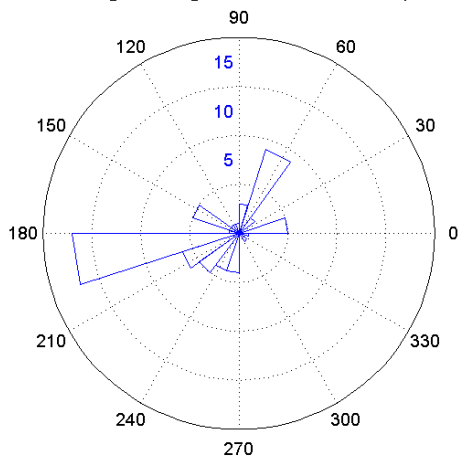


**Figure 3.14.** Condition #1 angle histogram shows dHL-60 cells migrated randomly when there is no fMLP present in the chemotaxis device

Instantaneous Angle Histogram at t = 60 minutes (Condition #2)

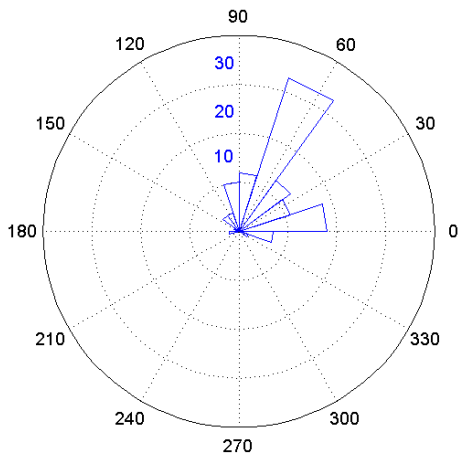


**Figure 3.15.** Condition #2 angle histogram shows dHL-60 cells migrated with a median angle of  $42^\circ$  in the direction of the gradient when fMLP is incorporated into the collagen gel

Instantaneous Angle Histogram at t = 60 minutes (Condition #3)

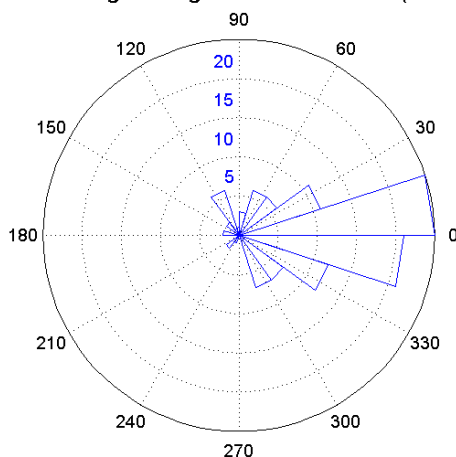


**Figure 3.16.** Condition #3 angle histogram shows dHL-60 cells migrated with a median angle of 7.8° degrees in the direction of the chemoattractant gradient when exposed to a stable, linear gradient in the device

For all three test conditions, the CI was calculated using each cell's position at 0 and 60 minutes and then averaged for each test condition. For condition #1 (64 cells), #2 (114 cells), and #3 (109 cells), the mean CI was calculated to be -0.3862, 0.4518, and 0.6479, respectively (outliers identified in MATLAB (see **Figure 3.17**) were not excluded in the mean CI calculation). A Wilcoxon rank sum test was used to determine if the difference between the three test conditions were statistically significant ( $\alpha = 0.05$ ). When condition #2 and #3 were compared to condition #1, the p-values were much less than 0.001. This demonstrated that in the presence of fMLP, the dHL-60 cells migrated in a more directed manner. This is an expected result since dHL-60 cells will migrate in response to a chemoattractant. However, when condition #2 and #3 were compared, the p-value was much less than 0.001. This showed that although the dHL-60 cells migrated when fMLP was incorporated into the collagen gel (condition #2), the cells migrated in a significantly more directed manner when exposed to a stable, linear chemoattractant gradient generated by the device (condition #3).

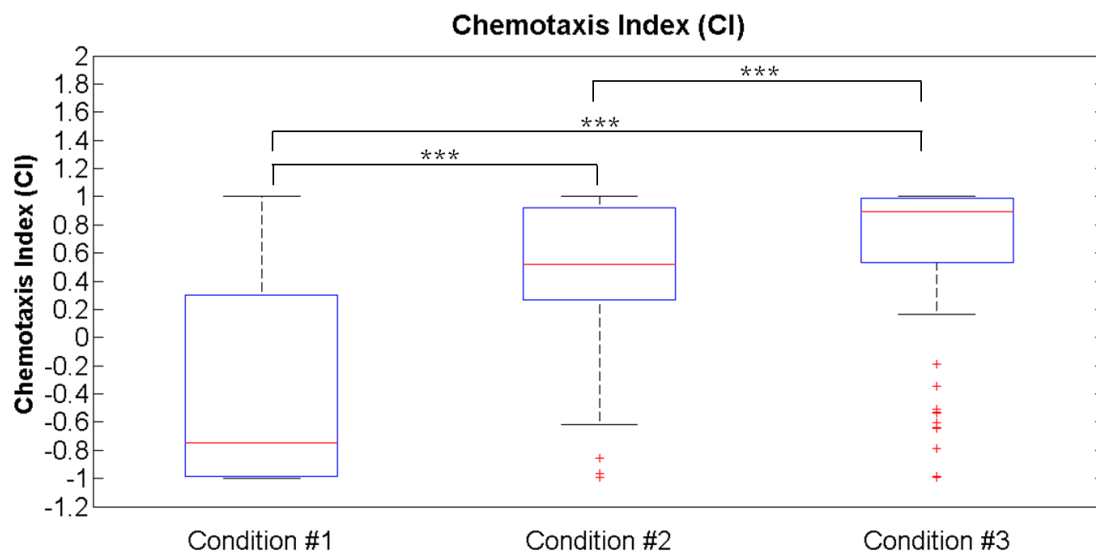


**Figure 3.17.** dHL-60 cells migrated in a significantly more directed manner when exposed to a stable, linear fMLP gradient generated by the device ( $p < 0.001$ )

## **4. DISCUSSION**

### **4.1. Characterization of the Concentration Gradient**

With 50 nM rhodamine in the source channel and media in the center and side channels, the device developed a stable linear gradient in approximately 300 minutes and maintained a stable gradient for at least 200 minutes. In order to decrease the amount of time needed to generate a stable gradient, 25 nM rhodamine was placed into the center channel. As a result, a stable gradient was generated in approximately 40 minutes and remained stable for at least 80 minutes.

However, the amount of time needed to form a stable gradient can also be reduced by decreasing the distance between the source and sink channels. This could enable more rapid formation of a stable gradient without incorporating chemoattractant into the center channel. The smallest achievable distance between the source and sink channel is dependent on the structural integrity of the agarose gel. If the distance between the channels is too small, the agarose channels may be disrupted when the hydrogel is removed from the stable. The distance between the source and sink channel will require optimization in order to minimize the distance while maintaining the channel features in the agarose gel.

### **4.2. Chemotaxis Studies**

The X and Y velocity, angular histograms, and CI values reported in this thesis demonstrated that the dHL-60 cells migrated in a direction that is parallel to the chemoattractant gradient. However, the observed migration velocities are lower compared to values reported in the literature, 0.2 – 0.25  $\mu\text{m/s}$ <sup>35</sup>. This could be due to several biochemical and mechanical parameters that may require optimization for future studies. First, the dHL-60 cells may need to be activated with fMLP prior to incorporation

into the collagen gel in order to observe more optimal chemotaxis behavior. In addition, the concentration of the collagen gel may need to be further optimized to obtain the most favorable *in vitro* 3D environment for dHL-60 cells. Lastly, increasing the number of cells analyzed could reduce the impact of outliers in the data analysis. This can be achieved by acquiring images throughout the thickness of the collagen gel (Z direction).

## 5. CONCLUSION

The purpose of this thesis was to develop and characterize a device which enabled the systematic study of the complex interplay between biochemical and mechanical processes that regulate neutrophil chemotaxis in 3D using readily available engineering tools and fabrication techniques. The system demonstrated that a model neutrophil cell type, HL-60, could be monitored for directional movement dictated by the chemoattractant, fMLP. The population of cells monitored was large enough to facilitate statistical analysis. Differentiated HL-60 cells migrated in a directed manner when exposed to fMLP for 60 minutes resulting in a mean CI of 0.6479 for 109 cells – demonstrating the device's utility. Furthermore, cell motility was observed for at least 60 minutes indicating the cells are viable in the device.

The device presented addresses many limitations with conventional flow based and diffusion based gradient generators while utilizing readily available manufacturing tools such as laser-cutting and 3D printing. The design and modular fabrication strategy for each component of the device allows for prototype to meet changing design requirements. In addition, the experimental set-up can easily be configured to accommodate different test conditions, allowing for the systematic study of biochemical and mechanical signals that may regulate cell migration such as different chemoattractants, cell types, and extracellular matrices enabling the study of many different cell migration pathways beyond the immune response.

Lastly, the device enables the study of cells in a more physiologically relevant environment since the cells can be encapsulated in a three-dimensional gel. This more closely resembles the native environment cells experience *in vivo* and can lead to more impactful knowledge in the field of 3D biology.

## 6. REFERENCES

- [1] Ridley, A. Cell Migration: Integrating Signals from Front to Back. *Science* 302, 1704-1709 (2003).
- [2] Janeway, C. *Immunobiology*. (Garland Science, 2005).
- [3] Karp, G. & Geer, P. *Cell and molecular biology*. (John Wiley, 2005).
- [4] Martinelli, R., Zeiger, A., Whitfield, M., Sciuto, T., Dvorak, A., Van Vliet, K., Greenwood, J. & Carman, C. Probing the biomechanical contribution of the endothelium to lymphocyte migration: diapedesis by the path of least resistance. *Journal of Cell Science* 127, 3720-3734 (2014).
- [5] Stroka, K. & Aranda-Espinoza, H. Neutrophils display biphasic relationship between migration and substrate stiffness. *Cell Motility and the Cytoskeleton* 66, 328-341 (2009).
- [6] Lämmermann, T. & Germain, R. The multiple faces of leukocyte interstitial migration. *Seminars in Immunopathology* 36, 227-251 (2014).
- [7] Steinwachs, J., Metzner, C., Skodzek, K., Lang, N., Thievensen, I., Mark, C., Münster, S., Aifantis, K. & Fabry, B. Three-dimensional force microscopy of cells in biopolymer networks. *Nature Methods* 13, 171-176 (2015).
- [8] Barthelat, F., Zavattieri, P., Korach, C., Prorok, B. & Grande-Allen, K. *Mechanics of biological systems and materials*.
- [9] Li, S., Guan, J. & Chien, S. Biochemistry and Biomechanics of Cell Motility. *Annual Review of Biomedical Engineering* 7, 105-150 (2005).
- [10] Van Haastert, P. & Devreotes, P. Chemotaxis: signaling the way forward. *Nature Reviews Molecular Cell Biology* 5, 626-634 (2004).
- [11] Horikawa, T., Norris, D., Yohn, J., Zekman, T., Travers, J. & Morelli, J. Melanocyte Mitogens Induce Both Melanocyte Chemokinesis and Chemotaxis. *Journal of Investigative Dermatology* 104, 256-259 (1995).
- [12] McCann, C., Kriebel, P., Parent, C. & Losert, W. Cell speed, persistence and information transmission during signal relay and collective migration. *Journal of Cell Science* 123, 1724-1731 (2010).
- [13] Kay, R., Langridge, P., Traynor, D. & Hoeller, O. Changing directions in the study of chemotaxis. *Nature Reviews* 9, 433-463 (2008).
- [14] Sallusto, F. & Baggiolini, M. Chemokines and leukocyte traffic. *Nature Immunology* 9, 949-952 (2008).
- [15] Millius, A. & Weiner, O. Chemotaxis in Neutrophil-Like HL-60 Cells. *Methods Mol Biol.* 571, 167-177 (2009).

- [16] Servant, G. Polarization of Chemoattractant Receptor Signaling During Neutrophil Chemotaxis. *Science* 287, 1037-1040 (2000).
- [17] Ridley, A. Cell Migration: Integrating Signals from Front to Back. *Science* 302, 1704-1709 (2003).
- [18] Cui, Y., Inanami, O., Yamamori, T., Niwa, K., Nagahata, H. & Kuwabara, M. FMLP-induced formation of F-actin in HL60 cells is dependent on PI3-K but not on intracellular  $Ca^{2+}$ , PKC, ERK or p38 MAPK. *Inflammation Research* 49, 684-691 (2000).
- [19] Hidalgo, M., Carretta, M., Teuber, S., Zárata, C., Cárcamo, L., Concha, I. & Burgos, R. fMLP-Induced IL-8 Release Is Dependent on NADPH Oxidase in Human Neutrophils. *Journal of Immunology Research* 2015, 1-14 (2015).
- [20] Kim, B. & Wu, M. Microfluidics for Mammalian Cell Chemotaxis. *Annals of Biomedical Engineering* 40, 1316-1327 (2011).
- [21] Boyden, S. The Chemotactic Effect of Mixtures of Antibody and Antigen on Polymorphonuclear Leucocytes. *Journal of Experimental Medicine* 115, 453-466 (1962).
- [22] Zigmond, S. Ability of polymorphonuclear leukocytes to orient in gradients of chemotactic factors. *The Journal of Cell Biology* 75, 606-616 (1977).
- [23] Servant, G. Polarization of Chemoattractant Receptor Signaling During Neutrophil Chemotaxis. *Science* 287, 1037-1040 (2000).
- [24] Lin, F. A Microfluidics-Based Method for Analyzing Leukocyte Migration to Chemoattractant Gradients. *Methods in Enzymology* 461, 333-347 (2009).
- [25] Jeon, N., Dertinger, S., Chiu, D., Choi, I., Stroock, A. & Whitesides, G. Generation of Solution and Surface Gradients Using Microfluidic Systems. *Langmuir* 16, 8311-8316 (2000).
- [26] Kim, S., Kim, H. & Jeon, N. Biological applications of microfluidic gradient devices. *Integr. Biol.* 2, 584 (2010).
- [27] Abhyankar, V., Lokuta, M., Huttenlocher, A. & Beebe, D. Characterization of a membrane-based gradient generator for use in cell-signaling studies. *Lab on a Chip* 6, 389 (2006).
- [28] Shamloo, A. & Heilshorn, S. Matrix density mediates polarization and lumen formation of endothelial sprouts in VEGF gradients. *Lab on a Chip* 10, 3061 (2010).
- [29] Cheng, S., Heilman, S., Wasserman, M., Archer, S., Shuler, M. & Wu, M. A hydrogel-based microfluidic device for the studies of directed cell migration. *Lab on a Chip* 7, 763 (2007).



- [30] Haessler, U., Kalinin, Y., Swartz, M. & Wu, M. An agarose-based microfluidic platform with a gradient buffer for 3D chemotaxis studies. *Biomedical Microdevices* 11, 827-835 (2009).
- [31] Liang, S., Xu, J., Weng, L., Dai, H., Zhang, X. & Zhang, L. Protein diffusion in agarose hydrogel in situ measured by improved refractive index method. *Journal of Controlled Release* 115, 189-196 (2006).
- [32] Ahearne, M., Yang, Y. & Liu, I. Mechanical Characterisation of Hydrogels for Tissue Engineering Applications. *Topics in Tissue Engineering* 4, (2008).
- [33] Wang, N. & Wu, X. Preparation and Characterization of Agarose Hydrogel Nanoparticles for Protein and Peptide Drug Delivery. *Pharmaceutical Development and Technology* 2, 135-142 (1997).
- [34] Millius, A. & Weiner, O. Manipulation of Neutrophil-Like HL-60 Cells for the Study of Directed Cell Migration. *Methods Mol Biol.* 591, 147-158 (2010).
- [35] Koyama, S., Narita, E., Shinohara, N. & Miyakoshi, J. Effect of an Intermediate-Frequency Magnetic Field of 23 kHz at 2 mT on Chemotaxis and Phagocytosis in Neutrophil-Like Differentiated Human HL-60 Cells. *International Journal of Environmental Research and Public Health* 11, 9649-9659 (2014).